Modeling of AC Losses in High-speed PMSM Windings: Methods, Challenges, and Prospects

Kaiwei He, Wenxiang Zhao, *Senior Member, IEEE*, Zhongze Wu, and Jinghua Ji

***Abstract*—High-speed permanent magnet synchronous motors (PMSMs) have recently been widely applied in various applications. However, due to the increased rotor speed and operating frequency increase, the winding AC losses rise substantially, posing risks to the safety operation. Accurate modeling of the AC losses has therefore become critical at the motor initial design stage. This paper reviews the main modeling methods for AC copper losses in PMSMs, including analytical methods, finite element methods, and hybrid modeling methods. The advantages and disadvantages of each method are analyzed in detail, and key issues in the modeling process are discussed. Finally, future research directions in AC copper loss modeling are explored, providing new insights for motor design and performance optimization.**

***Index Terms*—Permanent magnet synchronous motor, AC copper loss, Motor windings, High-speed motor.**

I. Introduction

CURRENTLY, with the increasing demand for high-speed permanent magnet synchronous motors (PMSMs) in electric vehicles, electric aircraft, and various industrial equipment, motor technology is gradually developing towards high-speed operation [1]-[4]. These high-speed motors possess advantages such as compact size, high power density, and low rotational inertia, which have been widely applied in various applications. However, as motor speed increases, the operating frequency also rises. The high-frequency operation significantly enhances the skin effect and proximity effect, resulting in an uneven cross-sectional current distribution inside the conductor. This uneven distribution increases the copper losses in the windings [5]. These losses, including circulating current effects caused by high-frequency operation, are collectively referred to as AC losses [6]. In contrast, in low-speed motors, the current frequency is relatively low, and the AC losses in the windings are almost negligible. The current is more evenly distributed across the conductor cross-section, and the copper losses are mainly composed of DC copper losses. Therefore, for high-speed motors, the AC losses in the windings have become one of the key factors limiting performance improvement. AC copper losses not only reduce motor efficiency but also tend to cause overheating of the windings, posing safety risks and affecting the reliability of the motor.

In recent years, the modeling and calculation of AC copper losses in high-speed PMSMs have become a research hotspot. Many studies have focused on exploring effective modeling methods to achieve accurate predictions of AC losses in the windings. At the same time, various optimization strategies have been proposed to reduce AC losses. These studies are of great significance for improving the performance and energy efficiency of high-speed PMSMs.

The modeling methods of AC copper losses in PMSMs can be categorized into three main types, i.e., analytical methods [7]-[19], finite element methods (FEM) [20]-[43], and hybrid modeling methods [29]-[37]. Early copper loss modeling was primarily based on analytical methods, estimating losses through electromagnetic field theory and mathematical formulas. However, with the increase in motor speed, various high-frequency effects also need to be further considered in analytical models. With the development of numerical computation methods, models based on FEM and other computational approaches have become the primary means of estimating motor copper losses. FEM can handle complex geometries and material nonlinearities, providing high accuracy. However, it also faces challenges such as complex modeling and long computation times, especially when fine copper loss modeling is required. To address this contradiction, hybrid modeling methods have been developed and widely applied, ensuring both calculation accuracy and reducing computation time effectively. In recent years, with the development of machine learning and big data technologies, machine learning-based copper loss models have also been proposed [38], [39]. These models use large amounts of simulation and experimental data to achieve rapid copper loss predictions through trained algorithms, offering new ideas and methods for AC loss modeling [40]-[42].

This paper will review the research conducted on AC copper loss modeling in recent years and discuss possible future research trends. The structure is organized as follows. In Section II, the types and mechanisms of AC copper losses

Manuscript received November 24, 2024; revised February 22, 2025; accepted April 02, 2025. Date of publication June 25, 2025; Date of current version May 16, 2025.

This work was supported in part by the National Natural Science Foundation of China under Grants 52025073 and 52377055. (*Corresponding Author*: *Wenxiang Zhao*)

K. W. He, and J. H. Ji are with the School of Electrical and Information Engineering, Jiangsu University, Zhenjiang 212013, China (email: hkw@stmail.ujs.edu.cn; jjh@ujs.edu.cn).

W. X. Zhao is with the School of Electrical and Information Engineering, Jiangsu University, Zhenjiang 212013, China, and also with the School of Electric Power Engineering, Nanjing Institute of Technology, Nanjing 211167, China (e-mail: zwx@ujs.edu.cn).

Z. Z. Wu is with the School of Electrical Engineering, Southeast University, Nanjing 210096, China (e-mail: zzwu@seu.edu.cn).

Digital Object Identifier 10.30941/CESTEMS.2025.00014

in PMSMs will be introduced. In Section III, AC copper loss models based on analytical methods, FEM, and hybrid models will be presented, respectively. Key issues in the modeling process, such as the influence of conductor types and material nonlinearities, will be discussed in Section IV. Future research directions and trends will be covered in Section V. Finally, a summary will be provided in Section VI.

II. Types of Losses in Conductors

A. Skin Effect

When AC current is applied on a single conductor, an alternating magnetic field is generated within the conductor. This alternating magnetic field induces eddy currents within the conductor. These induced currents flow in the opposite direction to the original current, partially canceling the current at the center of the conductor. As a result, the total current tends to concentrate on the surface of the conductor. This phenomenon is referred as the skin effect [8], as shown in Fig. 1.

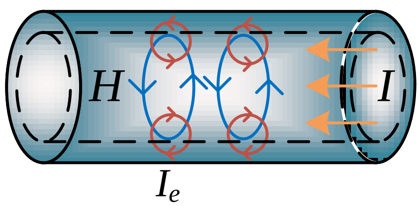

Fig. 1. Schematic diagram of skin effect.

Due to the skin effect, the effective conductive cross-sectional area of the conductor is reduced, which increases the equivalent resistance of the conductor. With the same current, the increased resistance results in a greater energy loss as heat. This additional loss caused by the skin effect is referred to as skin effect loss. The impact of the skin effect can be quantified by the skin depth δ, which is expressed as,

$$\delta=\sqrt{\frac{2\rho}{\omega\mu}} \tag{1}$$

where ρ is the resistivity of the conductor, μ is the permeability of the conductor, and $\omega=2\pi f$ is the angular frequency, with f representing the current frequency. The skin depth δ represents the depth at which the current density decreases to $1/e$ of its value at the surface of the conductor. When the current frequency is low, the angular frequency ω is small, resulting in a larger skin depth δ. This allows the current to be evenly distributed across the entire cross-section of the conductor, and the impact of the skin effect can be neglected. However, when the current frequency is high, the angular frequency ω increases, causing the skin depth δ to decrease, and the current is mainly concentrated on the surface of the conductor. The effective conductive cross-sectional area is reduced, and the equivalent resistance of the conductor is increased, thus making the skin effect more pronounced.

In addition, the diameter of the conductor also affects the extent of the skin effect. For conductors with large diameters under high-frequency condition, current distribution is significantly limited to the outer region, resulting in reduced material utilization and increased losses. Therefore, the impact of current frequency and conductor size on the skin effect are closely related and must be carefully considered when high-frequency motors are designed.

B. Proximity Effect

When AC currents are applied to adjacent conductors, an alternating magnetic field is generated around each conductor. These alternating magnetic fields interact with each other, inducing eddy currents in the neighboring conductors. These induced currents alter the current density distribution within the conductors, causing the current distribution across the conductor cross-section to become uneven. The uneven current distribution caused by electromagnetic interactions between adjacent conductors is referred to as the proximity effect [10], as shown in Fig. 2.

Similar to the skin effect, the proximity effect reduces the effective conductive cross-sectional area of the conductor, and the equivalent resistance is consequently affected. As a result, under the same current, heat loss will occur in the conductor. Under the high-frequency conditions, the current redistribution caused by the proximity effect becomes more pronounced, and the resulted losses can even exceed those caused by the skin effect.

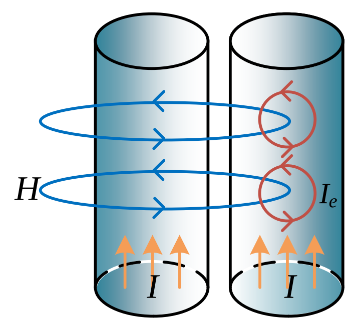

Fig. 2. Schematic diagram of proximity effect.

C. Circulating Currents

To reduce the eddy current losses caused by the skin effect and proximity effect under high-frequency conditions, it is common to use multiple strands of thin wires twisted together to form the windings. The cross-sectional area of the conductors is reduced by this approach, resulting in an increased ratio of skin depth to conductor radius, thereby weakening the skin effect. At the same time, as the conductor size decreases, the proximity effect is weakened, which reduces the additional losses caused by current redistribution [10].

The twisted stranded windings introduce new challenges. Due to the difference in self-inductance and mutual inductance in stranded coils, and hence the voltage potential difference, the current density distribution within the turns become uneven. The voltage potential differences induced additional current loops within conductors, is defined as the circulating currents. These circulating currents lead to additional losses, known as circulating current losses, and may cause localized overheating, thereby affecting the performance and reliability of the motor.

To address the circulating currents issue, Litz wire is commonly used. Litz wire consists of multiple insulated thin strands twisted together according to a specific pattern, ensuring that the spatial position of each strand periodically changes within the winding. Therefore, the path length and electromagnetic environment of each strand are averaged throughout the entire winding. This configuration eliminates the conditions necessary for circulating current formation, effectively reducing circulating current losses. Moreover, the benefits of thin conductors in mitigating the skin effect and proximity effect are preserved, whilst the issue of circulating currents in parallel windings is avoided. Therefore, the goal of reducing AC losses under high-frequency conditions is achieved.

In PMSMs, the leakage magnetic field within the stator slots is formed by the combined effects of the magnetic field generated by the PM and the magnetic field generated by the armature current. These leakage magnetic fields create a complex electromagnetic field distribution within the stator slots, which has a significant impact on the AC losses in the windings. Typically, the leakage field within the slots is primarily determined by the armature magnetic field, resulting in a significant effect on the losses.

Moreover, the magnetic field distribution within different areas of the stator slots is uneven. Near the slot opening, the leakage flux density is particularly significant.

The low magnetic reluctance near the slot opening leads to flux leakage into the air gap, resulting in a strong magnetic field in this region. The intense leakage magnetic field induces substantial eddy currents in the conductors, significantly increasing the AC losses in the conductors. Consequently, the conductor losses near the slot opening are usually the most severe and contribute substantially to the overall losses.

III. AC Loss Modeling Method

A. Analytical Methods

Analytical models can be categorized into three types based on different calculation variables, as shown in Fig. 3.

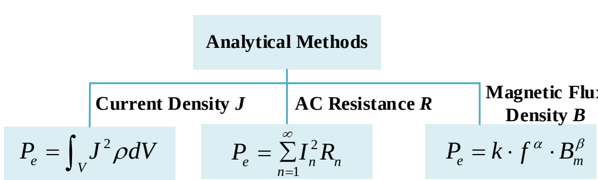

Fig. 3. Classification of analytical models.

In the modeling of AC copper losses in multi-layer windings, [11] demonstrated the orthogonality between the skin effect and the proximity effect. The principle of orthogonality states that the skin effect and the proximity effect are independent of each other in AC losses and can be calculated separately and then superimposed. This greatly simplifies the analysis process. The skin effect arises from the uneven distribution of alternating current within the conductor, while the proximity effect is caused by the influence of magnetic fields generated by surrounding conductors on the current distribution. The orthogonality of these two effects is utilized in the improved model to achieve precise calculations of AC losses in multi-layer windings across different frequencies.

$$P_{\mathrm{cu}} = \frac{1}{2\sigma}\int_A \left(J_{\mathrm{se}} J_{\mathrm{se}}^* + J_{\mathrm{pe}} J_{\mathrm{pe}}^*\right) \mathrm{d}A = \left(P_{\mathrm{se}} + P_{\mathrm{pe}}\right) \tag{2}$$

where J_{se} is the current density caused by skin effect in the conductor, and J_{pe} is the current density caused by proximity effect. σ is the conductivity of the winding material. A is the cross-sectional area of the conductor.

For the skin effect, the AC resistance can be calculated using the following formula:

$$P_{\mathrm{se}} = \frac{1}{2} R_{\mathrm{skin}} I^2 \tag{3}$$

where I represent the peak current, and R_{skin} is the equivalent resistance of the conductor under the skin effect.

For the proximity effect, the loss can be calculated using the following formula:

$$P_{\mathrm{pe}} = GH^2 \tag{4}$$

where, H is the peak value of the external magnetic field. The expression for G depending on the shape of the conductor. For round conductors:

$$G = \frac{-2\pi\gamma}{\sigma} \frac{ber_2\gamma ber'\gamma + bei_2\gamma ber'\gamma}{ber^2\gamma + bei^2\gamma} \tag{5}$$

while for flat conductors:

$$G = \frac{\frac{\sqrt{\pi}}{2} d\xi}{\sigma} \frac{\sinh\xi - \sin\xi}{\cosh\xi + \cos\xi} \tag{6}$$

where d is the conductor diameter. $\gamma = d/\left(\delta\sqrt{2}\right)$. $\xi = \sqrt{\pi} d / 2\delta$. ber_n and bei_n represent the real and imaginary parts of the *n-th* order Bessel function of the first kind.

The losses caused by the skin effect and proximity effect can be calculated by (3) and (4), respectively. These losses are then combined to obtain the total AC losses.

[12] proposed an analytical method for eddy current loss based on a subdomain field model. This model introduces the influence of tooth-tip effects and uses Fourier series to handle spatial harmonics, providing an accurate description of eddy current loss distribution. The electromagnetic field distribution is solved by dividing it into different subdomains, allowing this model to be applied to single-layer, dual-radial-layer, and dual-axial-layer winding structures. The winding distribution and current density function are shown in Fig. 4. AC copper losses are effectively predicted under various operating conditions:

$$P_{\mathrm{cu}} = \frac{\omega_{\mathrm{r}} l_{\mathrm{a}}}{2\pi\sigma} \int_0^{2\pi/\omega_{\mathrm{r}}} \int_{r1}^{r2} \int_{\alpha 1}^{\alpha 2} J_t^2 r \mathrm{d}r \mathrm{d}\alpha \mathrm{d}t \tag{7}$$

where r_1 and r_2 are the inner and outer radii of the stator, α_1 and α_2 are the circumferential positions of the conductors. ω_{r}

is the rotor rotational speed. l_a is the axial length.

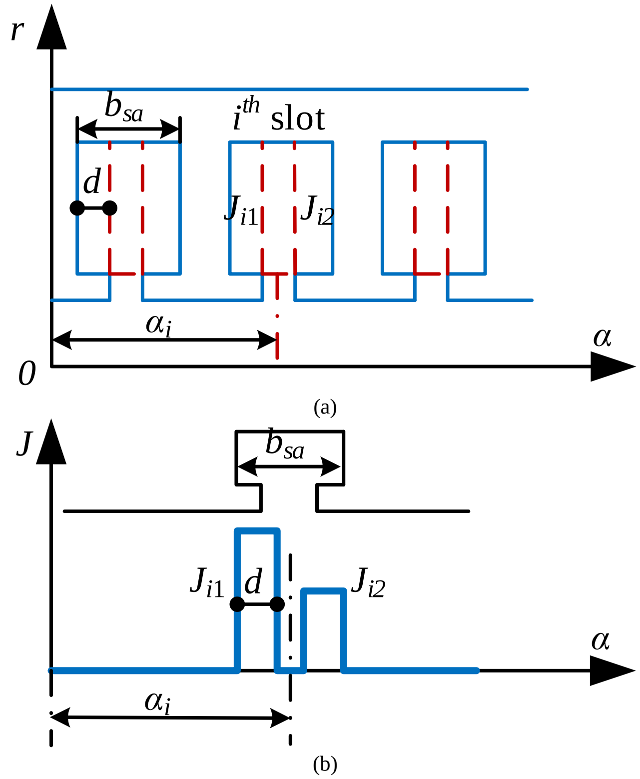

Fig. 4. Two-circumferential-layer winding. (a) Alternative winding layouts. (b) Current density function [12].

Furthermore, [13] proposed a new analytical model for eddy current loss that combines subdomain modeling techniques with a system of ordinary differential equations (ODEs):

$$[\mathrm{M}_{\mathrm{sc}}]\cdot\left[\frac{\mathrm{d}I}{\mathrm{d}t}\right]+[\mathrm{M}_{\mathrm{ph}}]\cdot\left[\frac{\mathrm{d}I_{\mathrm{ph}}}{\mathrm{d}t}\right]+[R]\cdot[I]=[U]-[E] \tag{8}$$

where $[\mathrm{M}_{\mathrm{sc}}]$ is strands inductance matrix. $[\mathrm{M}_{\mathrm{ph}}]$ is the inductance matrix between SCs and machine phases. The eddy current loss can be evaluated using:

$$P_{\mathrm{cu}}=\sum_n I_n^2 R_n \tag{9}$$

This method significantly reduces computation time through the combined application of conductor segmentation and equivalent circuits, enabling accurate calculation of eddy current losses in conductors with complex geometries.

[14] proposed an analytical method for calculating the AC resistance and reactance of motor windings in ferromagnetic slots. [15] discretizes the slot structure into multiple layers, based on which the magnetic field governing equations are established. The Poynting theorem is applied to calculate the complex power entering the conductor, allowing the effective resistance and reactance of the windings to be determined.

[16] proposed a model for the AC losses in high-frequency motor windings composed of large cross-section conductors. A dimensionless AC loss factor α is defined in this model. The factor combines the characteristic dimensions of the conductor, the conductor filling factor within the slot, and the conductor ampere-turns ratio to accurately evaluate AC losses in large cross-section conductors under high-frequency conditions. This method has shown results highly consistent with FEM in experimental validation. The effect of temperature changes on conductivity is considered through the coupling of electromagnetic and thermal models, enabling an accurate description of AC losses in windings under different frequencies and temperatures.

[17] proposed a precision-enhanced algorithm for the calculation of slot leakage inductance in double-layer windings. By correcting the simplified assumptions in traditional analytical methods, the accuracy of self-inductance and mutual inductance coefficient calculations for double-layer windings and arbitrary-shaped semi-closed slots has been improved. This model uses an energy method to calculate the magnetic energy within the slot region. By applying two correction formulas, results close to those obtained by FEM were achieved.

The analytical modeling of circulating current losses is typically based on the differences in self-inductance and mutual inductance caused by the uneven distribution of current in the windings. These differences lead to an imbalance in electromotive forces between parallel conductors, resulting in circulating currents. Analytical modeling methods are often built upon the principles of electromagnetic induction. Self-inductance, mutual inductance, and electromotive force relationships are combined with equivalent circuit models to describe electromagnetic phenomena within the motor.

[18] proposed an analytical modeling method for circulating current losses in the PMSMs. This method employs the subdomain approach combined with ODEs to solve the equivalent circuit, significantly improving computational efficiency. The equivalent circuit model is shown in Fig. 5. This is particularly advantageous in the design phase when evaluating winding losses and optimizing designs, offering a substantial time advantage over FEM.

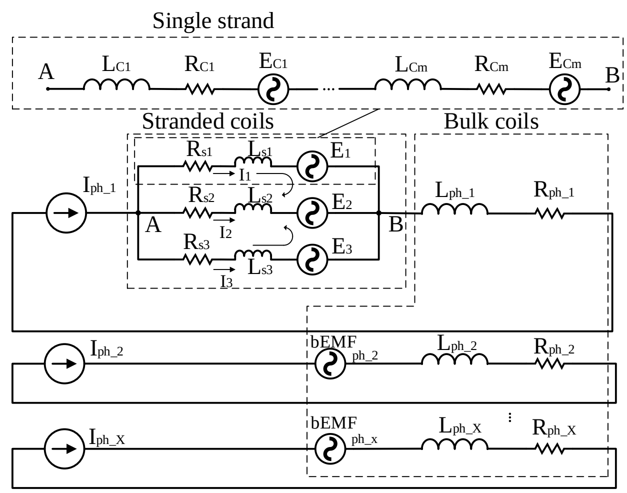

Fig. 5. Equivalent circuit structure [18].

[19] proposed a method for statistically analyzing circulating current losses in random wound motors using the Monte Carlo method, focusing on addressing the issue of circulating current losses caused by the random positioning of

conductors in the windings.

The analytical methods of AC loss modeling are summarized in Table I.

[12]-[16] all focused on the analytical model of eddy current loss, [12], [13], [15] and [16] only considered the eddy current loss model under the action of armature. [13] considered the eddy current loss under the load condition of the motor. Meanwhile, due to the time-domain analysis of the model, the loss under various current excitation can be considered in this paper. The model in [14] and [16] can be applied to a variety of trough structures. [15] has strong application value for large area copper wire. The model in [18] considers the modeling of circulating current loss, and still performs well under harmonic excitation.

In summary, analytical methods often have higher computational efficiency than numerical simulations (such as FEM). When dealing with conventional motor design problems, the analytical method can provide preliminary results quickly and provide preliminary reference. Meanwhile, analytical methods are often based on simplified physical models that provide an intuitive understanding of the loss mechanism. By simplifying assumptions about electromagnetic phenomena, analytical methods can quickly estimate losses without the need for complex meshing and boundary condition setting. In addition, it does not rely on a large number of input parameters, but more on physical characteristics (such as conductivity, frequency, etc.). It possible to conduct preliminary loss assessment in the absence of detailed experimental data. Due to the simplified assumption, the accuracy of the method is also affected to a certain extent.

B. FEM

FEM adopts a numerical computation approach, discretizing the solution domain into a mesh and solving the electromagnetic field distribution numerically. This method can accurately account for complex geometries, material nonlinearities and anisotropies, as well as the effects of boundary conditions, making it suitable for precise simulations in complex electromagnetic environments.

Commercial FEM software calculates eddy current losses primarily by relying on current density computations. From a numerical perspective, FEM calculates eddy current losses through magnetic vector potential.

[20] proposed a fast eddy current loss calculation method based on FEM, particularly suitable for calculating AC winding losses in large-scale design optimizations. Compared with traditional methods, this approach significantly improves computational efficiency by simplifying coil modeling and utilizing flux mapping techniques, while also considering the interactions between magnetic saturation and rotor dynamic/static magnetomotive forces.

[21] introduced a novel 3D FEM and analytical hybrid method for calculating AC winding losses in PMSMs. Compared to traditional 2D FEM methods, this approach better handles the leakage magnetic effects at the winding end, thus improving the accuracy of loss estimation.

When modeling circulating current losses using FEM, it is necessary to construct an external circuit model to clarify the distribution of parallel strands in the windings.

[22] conducted a detailed analysis of circulating current losses in the parallel conductors of windings in PMSMs, simulating the current distribution in each conductor using FEM. The study highlighted that circulating current losses are significantly higher than traditionally estimated copper losses. A strategy is proposed to reduce circulating current losses by decreasing the number of parallel conductors. The proposed optimization strategy was experimentally validated.

When copper loss is modeled using FEM, individual conductors must be modeled. The model’s meshing is complex and needs to be simplified. The loss accuracy calculated by 5 modeling methods is compared in [23]. Fig. 6 shows 5 FEM modeling models. Meanwhile, this paper investigated methods for reducing the AC winding losses in high-frequency motors by precisely controlling the placement of conductors within the slots. The study employed the 3D printing technology to achieve precise conductor placement. Experimental results showed that by positioning the conductors away from the high-leakage flux areas near the slot opening, and hence AC losses were significantly reduced. Additionally, it developed an automated conductor placement algorithm to further optimize winding structures and reduce losses.

TABLE I
ANALYTICAL METHODS FOR AC LOSS MODELING

Reference	Eddy Current Loss Calculation Method	Calculation Target	Key Features
Ref. [11]	Current density *J*	Eddy current loss	Orthogonality of skin and proximity effects for multi-layer windings.
Ref. [12]	Current density *J*		Subdomain field model with tooth-tip effects and Fourier series for spatial harmonics.
Ref. [13]	Equivalent resistance *R*		Combines subdomain modeling with ODEs for complex conductor geometries.
Ref. [14]	Electric field intensity *E*		AC resistance and reactance calculation for windings in ferromagnetic slots.
Ref. [15]	Equivalent resistance *R*		Uses Poynting theorem for effective resistance and reactance in layered slot structures.
Ref. [16]	Magnetic field intensity *B*		High-frequency AC loss factor considering temperature effects in large cross-section conductors.
Ref. [17]	Magnetic dipole moment	Circulating current loss	Enhanced slot leakage inductance calculation using energy method and correction formulas
Ref. [18]	Equivalent resistance *R*		Efficient calculation of circulating current losses using subdomain and ODEs.
Ref. [19]	Electric field intensity E		Monte Carlo method for circulating current loss in random wound motors.

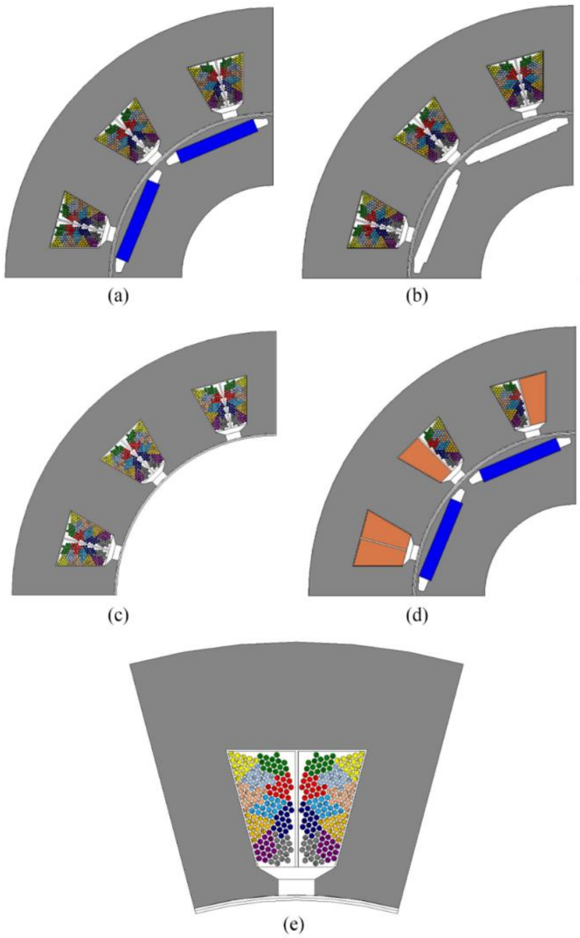

Fig. 6. Comparison of models for simplification [23]. (a) Quarter model. (b) No permanent magnet model. (c) No rotor model. (d) Single coil strand modeling model only. (e) Single slot model.

[24] used FEM to evaluate the impact of various frequencies and conductor arrangements on proximity losses. The impact of FEM model complexity and various testing conditions on simulation accuracy are also investigated. [25] examined the copper losses in a 5 MW high-speed PM machine with form-wound windings. Through experimental validation and FEM simulations, the study calculates copper losses across the machine entire speed range.

A practical transposition approach is proposed in [26] proposes for high-speed motor windings to suppress AC copper loss. FEM is used to analyze the skin effect and proximity effect on copper loss under high-frequency conditions, particularly focusing on the distribution of circulating current losses. Simulation results demonstrate that the approach effectively balances the magnetic linkage among parallel strands in random windings, significantly reducing circulating current losses.

[27] focuses on modeling AC copper losses in PMSMs with hairpin windings by developing an advanced d-q axis model that accurately represents losses from armature and field excitation. The model employs a magneto-static FEM to efficiently calculate AC copper losses, separating components due to skin and proximity effects. Compared to transient FEM, using the static FEM with the frozen permeability approach improves computational efficiency.

[28] used FEM to investigate current density distribution and AC losses across five winding configurations, including traditional hairpin winding and hybrid transposed hairpin winding (HTHW), as shown in Fig. 7. The HTHW incorporating a Litz wire in conductor layers near the slot opening. The loss comparison results under different frequency conditions indicate that HTHW effectively suppresses losses at the high-frequency operation.

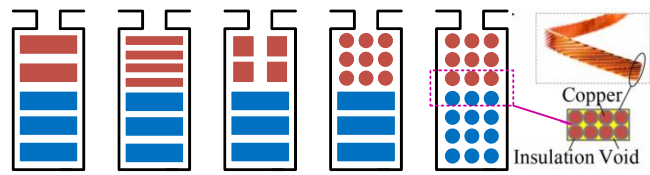

Fig. 7. Five schemes of HW [28].

The FEM of AC loss modeling are summarized in Table II. [22]-[23] and [25] compared various conductor arrangements and the number of parallel wound conductors by FEM, and studied the means of reducing AC copper consumption by conductor arrangement. The fast and low loss design method of [20] is suitable for the general motor design evaluation stage. The model proposed in [24] and [26] is suitable for loss estimation of high-speed motor. The effect of PWM harmonics on loss is considered in [25].

TABLE II
FEM FOR AC LOSS MODELING

Reference	Model Dimension	Calculation Target	Key Features
Ref. [20]	2D FEM	AC copper loss	Fast eddy current loss calculation with coil modeling simplification and flux mapping for large-scale optimizations.
Ref. [21]	3D FEM		Handles leakage magnetic effects at winding end to improve loss estimation accuracy.
Ref. [23]	3D FEM		Reduces AC losses through conductor positioning near slot opening using 3D printing and automated placement algorithm.
Ref. [24]	2D FEM		Evaluates impact of frequencies and conductor arrangements on proximity losses, considers FEM model complexity.
Ref. [25]	3D FEM		Calculates copper losses across full speed range of a high-speed 5.0 MW machine.
Ref. [26]	2D FEM		Using FEM to balance the magnetic linkage among parallel strands in random windings, significantly suppressing AC copper loss in high-speed motors.
Ref. [43]	2D FEM		A HTHW is proposed and compared with traditional winding structures using FEM, demonstrating a reduction in AC loss.
Ref. [27]	2D FEM		Using the static FEM with the frozen permeability approach improves computational efficiency.
Ref. [22]	3D FEM	Circulating current loss	Simulates circulating current losses in parallel conductors, validated optimization strategy by reducing conductor count.

The advantages of modeling by FEM in AC copper loss are mainly reflected in high precision and comprehensive consideration of complex electromagnetic effects. FEM captures skin, proximity and circulating current effects precisely, making it suitable for high frequency and high current applications. In addition, FEM can effectively simulate different winding topologies, which makes it irreplaceable in the study of high-performance motor design, loss optimization, and new winding structures (such as card winding, transposition winding). However, the disadvantages of FEM are obvious. The large amount of computation and long solving time are the main problems, especially at high frequencies, the grid needs to be refined to ensure the calculation accuracy, which leads to high computing resource consumption.

C. Hybrid Model

Hybrid modeling methods combines the methods such as FEM, analytical methods, and equivalent circuit model to achieve a balance between accuracy and computational speed.

In [29], the linear time-harmonics FEM is first used to perform an accurate analysis of the leakage magnetic field within the stator slots. The frozen differential permeability method is applied to consider the harmonics effect.

The magnetic field intensity in the conductor located in the *m*-th row and *n*-th column, caused by the *h*-th PWM harmonic of the *s*-th frozen step at order *v*, is given by:

$$B(m,n,s,h) = F\Lambda_0 = I_{\mathrm{vh}} \frac{N\Lambda_0}{a} \sin(v\omega t + \phi) \tag{10}$$

where I_{vh} is the amplitude of the PWM harmonics. N is the number of turns. Λ_0 is the permeance. F is the MMF of the slot leakage. ϕ is the phase of the current. ω is the fundamental angular velocity.

Next, the magnetic field data within the slots, predicted by FEM, is applied as the input for the analytical method. The current density in the conductor was derived considering high-frequency effects, taking into account both the skin effect and proximity effect.

$$\begin{aligned} J_{\mathrm{se}} &= \frac{I_0 j^{\frac{3}{2}} k J_0\left(j^{\frac{3}{2}} kr\right)}{2\pi r_{\mathrm{c}} J_1\left(j^{\frac{3}{2}} kr_0\right)} \\ J_{\mathrm{pe}} &= \frac{2H_0 j^{\frac{3}{2}} k J_1\left(j^{\frac{3}{2}} kr_0\right)}{J_0\left(j^{\frac{3}{2}} kr_0\right)} \sin\varphi \end{aligned} \tag{11}$$

where I_0 is the AC current, r_{c} is the radius of the conductor, H_0 is the strength of the external magnetic field. φ is the angle relative to the magnetic field.

The analytical method enables a rapid estimation of AC losses in the windings. In this hybrid model, the influence of PWM harmonics is considered while ensuring both computational accuracy and speed.

[30] proposed a method combining FEM analysis with basic circuit equations to estimate current distribution among parallel strands in low-voltage high-speed machines. This approach is designed for 3D geometries and considers the influence of strand twisting on current distribution, while minimizing computational resource usage. [31] utilizes a FE subdomain method to calculate the leakage magnetic field distribution within the slots, which is then substituted into analytical equations to compute the eddy current losses in the windings. [32] combines two formulas to accurately account for non-sinusoidal flux density effects, providing higher precision compared to traditional methods.

When modeling circulating current losses in parallel conductors, hybrid modeling methods typically rely on the combination of equivalent circuit models with FEM or analytical models. In the hybrid model, slot leakage field analysis and circulating current calculation are separated. The magnetic field model within the slots is constructed using FEM or analytical models to obtain the magnetic field distribution, current density distribution, or inductance distribution. The FEM model is simplified, reducing computational costs.

Equivalent circuit models are introduced to address limitations in electromagnetic field models, describing the electrical characteristics and interconnections between parallel conductors. The equivalent circuit model can include the resistance, inductance, and coupling parameters of the conductors, simulating the current distribution and circulating current paths among the conductors. The electromagnetic field data from the FEM model are combined with the equivalent circuit model to form a field-circuit coupled model. This model accurately simulates the loss mechanisms of circulating currents.

[33] proposed a semi-analytical method for modeling AC copper losses in stranded windings, considering the circulating current effect among parallel conductors. This method first solves the current in each conductor through an analytical circuit model, then combines the analytical model to calculate the current density distribution within the conductor, thereby estimating the AC losses in the windings.

In addition to traditional hybrid modeling methods, data-driven, multiphysics-coupled, and machine learning-based models are also increasingly emerged and applied in AC copper loss modeling. These methods provide new approaches to solving complex motor loss problems.

[34] utilized a time-space transformed computationally efficient FEM to extract slot leakage fields and incorporating an automated conductor allocation method. The circuit model is shown in Fig. 8. It enhances flexibility and accuracy in multi-phase windings and various conductor bundling configurations by automatically assigning conductor positions in the analytical model.

[35] introduces an electromagnetic network method based on the equivalence of local magnetic fields to calculate transient circulating current losses in large synchronous compensators. The discrete sections of parallel-wound transposition strands of stator windings are shown in Fig. 9. By reducing the 3D nonlinear transient problem into a combination of 2D nonlinear and 3D local linear problems, this method effectively considers the main field and magnetic saturation effects, making it suitable for different transposition structures.

[36] presents an improved winding loss calculation method

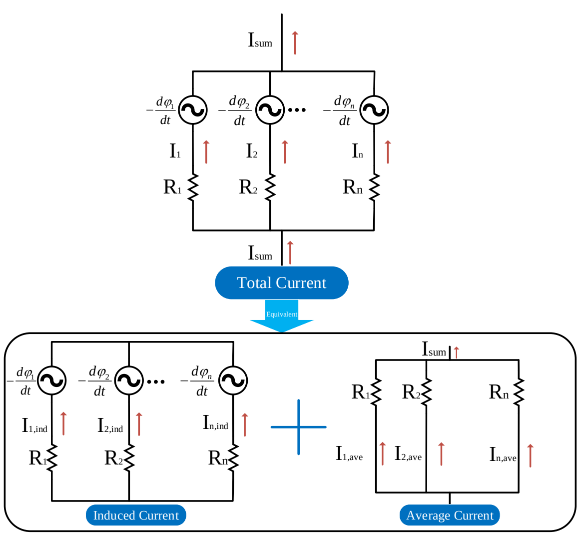

Fig. 8. Circuit model with n parallel strands [34].

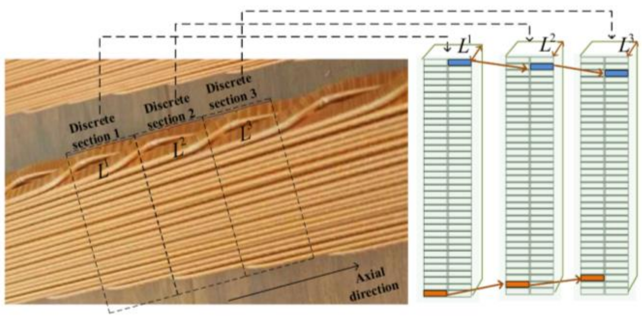

Fig. 9. Schematic diagram of discrete sections of parallel-wound transposition strands of stator windings [35].

based on Bessel functions, suitable for round conductor layer windings. By converting a constant magnetomotive force into a frequency-dependent magnetic field and introducing geometric factors to refine proximity effect calculations, this method effectively addresses interactions between conductors and improves accuracy in loss estimation.

[37] developed a multiphysics model that combines magnetic, thermal, and mechanical modeling to calculate copper losses, highlighting the role of multiphysics coupling in motor design optimization. The results were compared to a FEM design and showed good accuracy and the speed is increased by a factor of 5.

The hybrid models of AC loss modeling are summarized in Table III. The model proposed in [30], [33]-[35] focuses on modeling of circulating current loss caused by parallel stranded winding. [33] and [35] focused on the influence of wire transposition on loss. Multiphysics modeling is the trend of motor design. [37] adopted a multiphysical field model to model copper loss and considered the interaction between thermal field and loss. When the armature current is small, the armature winding has little influence on the leakage magnetic field distribution in the slot. The modeling method of combining static FE and analytical method proposed in [34], [29] can quickly calculating AC copper loss.

The hybrid model combines the advantages of analytical and numerical methods in AC copper loss modeling, aiming to strike a balance between computational accuracy and efficiency. However, the hybrid model also has some limitations. The development and implementation of these models can be complex due to the need to combine analytical and numerical solutions.

The comparison of the three methods is shown in the Table IV.

TABLE III
HYBRID MODEL FOR AC LOSS MODELING

Reference	Hybrid Method	Calculation Target	Key Features
Ref. [29]	FEM + analytical	Eddy current loss	Uses frozen differential permeability method to include harmonics in FEM for accurate slot magnetic field distribution.
Ref. [31]	FEM + analytical		Calculates slot leakage magnetic field for eddy current loss estimation.
Ref. [36]	FEM + analytical		Refines proximity effect with geometric factors and frequency-dependent magnetic field
Ref. [34]	FEA+ circuit	Circulating current loss	Utilizing FEM to extract slot leakage fields and incorporating an automated conductor allocation method.
Ref. [35]	Electromagnetic network Method + analytical method		Combines 2D nonlinear and 3D linear problems, accounting for main field and magnetic saturation.
Ref. [30]	FEM + circuit	AC copper loss	Estimates current distribution in parallel strands, accounting for strand twisting.
Ref. [33]	FEM + analytical		Considers circulating current effect in stranded windings for AC loss.
Ref. [37]	Multiphysics coupling		Highlight's role of multiphysics coupling in copper loss estimation and motor design.

TABLE IV
COMPARISON MODELS IN AC COPPER LOSS CALCULATION

Method	Computational Cost	Calculation accuracy	Advantages	Disadvantages	Applicability	Related references
Analytical method	+	+	Provides an intuitive understanding of loss mechanisms through simplified physical models.	Difficult to consider complex electromagnetic effects such as circulating currents, nonlinear materials, and special winding structures.	Preliminary assessment of traditional motor designs	Refs. [11]-[19]
FEM	+++	+++	Ability to adapt to complex structures and handle complex geometry and material properties.	Computational cost increases significantly with higher frequencies and finer meshes.	High-frequency and high-current applications, complex motor designs.	Refs. [20]-[43]
Hybrid model	++	++	Combines the strengths of analytical and numerical methods to balance accuracy and efficiency.	The process of model construction and verification is complex and requires a combination of methods.	Motor design stage and motor performance verification stage	Refs. [29]-[37]

IV. KEY ISSUES IN THE MODELING PROCESS

A. Winding Types and Modeling Characteristics

The conductor types that mainly used in motors can be categorized into three types: stranded wire, flat wire, and Litz wire, as shown in Fig. 10.

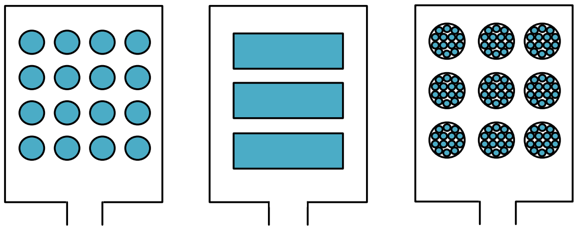

Fig. 10. Wire type. (a) Stranded Winding. (b) Flat Wire Winding. (c) Litz Wire Winding.

1) Stranded Winding

Stranded windings are composed of multiple thin wires twisted together in a specific pattern to form a single conductor. These thin wires are usually insulated to prevent electrical contact between the strands. Stranded windings are widely used in motors that require flexibility and good heat dissipation performance.

In non-parallel stranded winding, each strand of wire is independent and not connected in parallel, so the main losses to consider are eddy current losses caused by the skin effect and proximity effect. Since there are no loops formed between the wires, circulating current losses can be ignored.

In parallel stranded winding, multiple strands of wire are wound in parallel, and voltage differences between the wires may arise, leading to the generation of circulating currents. Circulating current losses thus become the primary source of losses and must be a key consideration in the modeling process [11].

Due to the small diameter, large quantity, and variable positions of the conductors in the electromagnetic field, precise consideration of their positions and interactions is required in the modeling process. This increases the complexity of the model and demands higher accuracy in modeling.

2) Flat Wire Winding

Flat wire windings use conductors with a rectangular or flat cross-section. These conductors enable compact filling of the slot space, improving space utilization compared to round wires. Flat wire windings are commonly used in motors requiring high power density and good heat dissipation performance, such as electric vehicle drive motors.

Due to the larger cross-sectional area of flat wires, eddy current losses caused by the skin effect and proximity effect increase under high-frequency conditions. Due to flat wire windings are typically not connected in parallel, the circulating current losses can be ignored [10]. There are four types of flat wire winding, Ipin, Hairpin, Xpin, and Swinding. Hairpin is currently the most widely used flat wire winding form, usually used in high power, high efficiency motors and frequency converters. The copper loss characteristics of the Hairpin winding and the stranded winding are shown in the Table V.

TABLE V
COMPARISON OF AC COPPER LOSS CHARACTERISTICS BETWEEN HAIRPIN WINDING AND STRANDED WINDING

Feature	Hairpin winding	Stranded winding
Ac loss sensitivity	Higher due to increased eddy current and proximity effects.	Lower due to smaller conductor area.
Slot filling factor	Higher, leading to better space utilization.	Lower, less efficient use of slot space.
Current distribution	More uniform.	Less uniform, with higher skin effect losses.
Harmonic sensitivity	More sensitive to harmonic currents, especially at high frequencies	Less sensitive

Flat wires have larger dimensions, regular shapes, fewer conductors, and a relatively simple electromagnetic field distribution. In modeling, certain simplifications can be made, such as approximating flat wires as continuous conductive regions, which reduces the required precision. The model construction is also relatively simple, reducing the computational load.

The simulation of AC copper with FEM model is time-consuming, and the modeling of Hairpin winding is relatively simple compared to that of a single conductor when modeling stranded winding. However, because the Hairpin winding is more sensitive to harmonic currents, especially at high frequencies. It is necessary to consider the influence of high frequency harmonics [43]. [27] using the freezing permeability method to addressed this issue. The nonlinear magnetostatic analysis is performed initially, followed by the calculation of the AC copper loss under the influence of the armature field and the excitation field individually. Finally, the AC copper loss resulting from the interaction of both fields is calculated using the actual current density for each MMF component. [44] calculated the magnetization at fundamental frequency by FEM, followed by the calculation of conductor loss using the partial element equivalent circuit. The models enhance efficiency compared to traditional FEM by effectively handling complex geometries while maintaining high accuracy.

3) Litz Wire Winding

Litz wire (stranded twisted wire) is composed of multiple thin, insulated wires twisted together according to a specific rule, with each strand periodically changing position along the length of the wire. Litz wire windings are suitable for high-frequency applications and can effectively reduce AC losses. They are commonly used in high-frequency transformers and high-speed motors.

Litz wire winding consists of multiple thin wires twisted together in a specific pattern. Due to the smaller conductor diameter, eddy current losses caused by the skin effect and proximity effect are reduced. Additionally, each strand periodically changes position along the axial direction, averaging the electromagnetic environment of each strand and reducing circulating current losses [45].

B. End Effect

In the modeling of AC copper losses in PMSMs, the end windings losses are often neglected in 2D models. 2D models can only describe the cross-sectional characteristics of the motor and cannot reflect the electromagnetic field distribution in the axial direction. In the end winding region, significant eddy current effects can arise due to high-frequency leakage flux. This has a considerable impact on the AC copper losses in the end windings.

The additional losses caused by high-frequency leakage flux in the end windings can be non-negligible in some high-speed or high-frequency motors. To improve the accuracy of AC copper loss models, end winding loss modeling needs to be extended from 2D models to 3D models to accurately simulate the electromagnetic field distribution in the end region. Through 3D model analysis, the leakage flux paths and eddy current losses in the end windings can be captured, enabling a more comprehensive and accurate assessment of the overall AC copper losses in the motor.

[46] studied the impact of the end region on eddy current losses by simulating the end magnetic field variations using the reaction-diffusion equation. [47] employed a 3D FEM to assess the impact of different end winding lengths on AC copper losses in high-speed stator flux-switching machines, demonstrating that the eddy current effects in the end winding region significantly increased losses. [21] proposed a 3D FEM and analytical hybrid method that carefully considered the effects of leakage flux in the end windings on current distribution and losses, effectively improving the accuracy of loss estimation. [48] improved the accuracy of 2D FEM by compensating for the leakage flux in the end windings through “scaling analysis”.

C. *Material Nonlinearity and Temperature Effects*

In PMSMs, the magnetization curve of the ferromagnetic materials in the stator and rotor cores is nonlinear, meaning that the magnetic flux density B no longer changes linearly with the magnetic field strength H. When the core reaches the saturation region, the permeability μ of the material decreases significantly. This reduction leads to an uneven magnetic flux density distribution, which in turn affects the electromagnetic field distribution around the conductors. The change in permeability directly influences the skin effect and proximity effect, making the current density distribution more complex.

Traditional analytical methods, such as those used by [49] and [50], usually assume that the permeability of the core is infinite and neglect saturation effects, implying that the motor operates at relatively low saturation levels. Due to these limitations, some analytical models have been proposed that account for the saturation effects. Certain analytical models consider the core saturation by segmenting the magnetization curve into linear sections or by using approximate methods with equivalent permeability. [51] and [52] approach the saturation effect through a saturation factor that equivalently extends the air gap length, a technique primarily applied to machines with relatively uniform flux paths. In [53] and [54], nonlinear subdomain models were introduced to address saturation, where the permeability of stator teeth and rotor poles is explicitly considered, contrasting with conventional models that assume infinite permeability. [55] and [56] calculates the saturation effects by adding equivalent current sheets to the stator teeth and yoke.

The equivalent magnetic network (EMN) method addresses saturation by calculating the permeability of different parts of the core. This method constructs a network of permeabilities, allowing the computation of magnetic field distribution in nonlinear cores while iteratively applying the material’s B-H curve, as described in [57]-[60]. [61] and [55] present hybrid models that combine the EMN model with a slot less flux density model for no-load and load conditions, respectively. The general solution of Maxwell’s equations is used to calculate the magnetic field distribution in the PM region and air gap, while EMN are used to obtain the magnetic field distribution in the slots and stator core.

Temperature rise leads to changes in the resistivity and permeability of materials, resulting in increased copper losses. The heat generated by electromagnetic losses causes the internal temperature of the motor to rise further, forming a cyclic process of thermal-electromagnetic interaction. This temperature increase not only affects the electrical and magnetic properties of materials but may also cause insulation material degradation, impacting the reliability and lifespan of the motor. Due to the coupling relationship between temperature and the electromagnetic field, magnetic-thermal coupling models have been proposed to accurately predict motor losses and temperature distribution during long-term operation [62]. These models consider the mutual influence of electromagnetic and thermal fields. Loss and temperature variations under actual operating conditions are simulated through iterative calculations.

D. *PWM Harmonic Supply*

As motor technology advances towards higher speeds and frequencies, the issue of current harmonics in drive systems has become increasingly prominent. The presence of current harmonics results in additional AC copper losses, electromagnetic interference, and may lead to increased motor vibration and noise, thereby affecting the motor’s performance and lifespan. To suppress harmonics and improve the efficiency and reliability of motor operation, inverters are typically used for power supply. However, PWM currents inherently contain high-frequency switching harmonic components, which exacerbate the skin effect and proximity effect, leading to increased AC copper losses in the windings. Due to the small-time steps required, accurately modeling the PWM mode as the voltage input in motor simulations demands a substantial computational effort.

For copper loss calculations under non-sinusoidal power supply, [29] compared the additional copper losses due to the skin effect in windings when using SVPWM and two-level PWM inverter supply strategies. The results indicated that the two-level PWM inverter supply strategy leads to higher skin effect losses in the conductors, which is detrimental to motor efficiency improvement.

[56] investigates the impact of varying PWM switching frequencies on harmonic losses and torque ripple in SPM motor systems. A 2D nonlinear time-stepping FEM is used to incorporates proximity effects in the conductors. Findings

indicate that motor performance is significantly impacted by switching frequency selection, and a balance between efficiency and torque ripple is required.

[63] studied and analyzed the AC copper losses in different winding types under PWM power supply. The study compared three different winding designs and used FEM to calculate the copper losses under pure sinusoidal current and PWM voltage supply conditions. The research found that the presence of high-frequency harmonic components in PWM supply significantly enhances the eddy effect in the windings. Additionally, hairpin windings were found to be more sensitive to high-frequency harmonics, resulting in higher copper losses.

[64] analyzed the effects of inverter characteristics such as switching frequency and modulation strategies on AC copper losses in motors. In the study, an 800 V two-level voltage source inverter was used, and space vector modulation (SVM) and various discontinuous PWM methods were compared for their impact on copper losses. The results indicate that discontinuous PWM methods reduce inverter switching losses compared to SVM but increase current harmonics, leading to higher copper losses in the motor. The study further analyzed the influence of switching frequency on losses, finding that higher switching frequencies reduce copper losses but increase inverter losses.

[65] proposed a semi-analytical method for quickly calculating conductor eddy current losses in motors powered by inverters. The model combines 2D magnetostatic FEM and high-frequency eddy current loss analytical formulas. The frozen permeability method is utilized to achieve fast calculation of PWM slot leakage magnetic fields. This method is suitable for the design and optimization of motor and inverter systems.

V. Research Outlook

A. Multi-physics Coupling Modeling

The physical fields within the motor are coupled and interact with each other. As the operating conditions of the motor change, various factors within the motor dynamically vary. By analyzing the coupling relationship between the magnetic field in the winding slots, the eddy current effect between conductors, and the winding temperature, the interactions among different physical fields are simulated. A multi-physical field coupling model is established to more accurately predict copper losses. At the same time, the layout and design of the windings are optimized. Non-uniform windings or segmented conductors are designed to reduce high-frequency losses by improving current distribution. For high-speed motors or high-frequency operating conditions, magnetic circuit structures with low magnetic reluctance and low harmonic distortion are designed to reduce additional copper consumption caused by magnetic field distortion.

B. Applications of Artificial Intelligence and Machine Learning

With the development of machine learning and big data technology, various loss models based on machine learning have also been proposed. Artificial intelligence technology has been widely used in the field of motor, such as fault diagnosis, condition monitoring, iron loss prediction, etc. Through a large number of simulation and experimental data, the training algorithm can achieve rapid prediction of loss, providing a new method for AC loss modeling [66]-[69].

[70] proposes a motor design system combining generative adduction network and vision Transformer. Based on three rotor topologies, geometric parameters are randomly generated, and the iron loss of the topology is generated by FEM. Input data such as geometry, current, and speed conditions are used, and a multilayer perceptron is employed to predict motor parameters and iron losses. [71] uses FEM simulation data to train deep convolutional neural networks in a supervised manner, learning the magnetic field distribution maps for various complex geometries, materials, and excitation topologies to achieve magnetic field prediction. [72] combines physical models with data-driven methods to establish a simplified lumped-parameter thermal network model for the stator windings and permanent magnets, and uses artificial neural networks to fit unmodeled characteristics and parameter variations. This approach achieves accurate estimation of stator and rotor temperatures while reducing computational load and parameter dependence. [73] employs a deep residual network for real-time estimation of motor temperatures. Through Bayesian optimization for automatic hyperparameter search, it enables continuous dynamic prediction of internal motor temperatures. [74] uses a large amount of iron loss data based on sinusoidal current excitation to establish a surrogate model via transfer learning, achieving iron loss prediction under PWM excitation and significantly improving computational efficiency under complex operating conditions. These studies demonstrate that through loss modeling, parameter estimation, and data correction, deep learning can effectively improve the accuracy and efficiency of motor performance prediction, providing new ideas and directions for AC copper loss modeling and analysis. By combining parallel computing and model order reduction techniques [75]-[77], and considering the dynamic variations of motor AC losses under complex operating conditions, real-time prediction and intelligent optimization of motor losses can be achieved in conjunction with control strategies.

VI. Conclusion

In this paper, the modeling methods for AC copper losses in the windings of PMSMs are systematically reviewed and summarized. The characteristics of different modeling methods are summarized.

Analytical methods improve computational efficiency by simplifying the physical model. However, due to the over-simplified material property, the accuracy of the model is reduced, making these methods unsuitable for high-saturated and complex topologies.

FEM allows for precise modeling of complex motor structures and simulation of intricate electromagnetic environments, achieving high computational accuracy. However, it requires substantial computational resources and is time-consuming due to its high computational demand.

Hybrid modeling methods are formed by combining analytical and FEM approaches. Equivalent circuits or semi-empirical formulas are introduced to enhance computational efficiency while maintaining accuracy. However, specific simplification strategies must be considered for different motor applications in hybrid modeling.

Additionally, due to the nature of AC losses, several key issues must be carefully addressed during the modeling process to improve model accuracy. This paper provides a valuable reference for selecting appropriate modeling methods in future research.

References

[1] J. X. Shen, X. F. Qin, and Y. C. Wang, "High-speed Permanent Magnet Electrical Machines — Applications, Key Issues and Challenges," *CES Trans. on Electr. Mach. and Syst.*, vol. 2, no. 1, pp. 23–33, Mar. 2018.

[2] Y. Zhao, D. W. Li, and T. H. Pei *et al*, "Overview of the Rectangular Wire Windings AC Electrical Machine," *CES Trans. on Electr. Mach. and Syst.*, vol. 3, no. 2, pp. 160–169, Jun. 2019.

[3] G. Gallicchio, M. D. Nardo, and M. Palmieri *et al*, "Surface Permanent Magnet Synchronous Machines: High Speed Design and Limits," *IEEE Trans. on Energy Convers*., vol. 38, no. 2, pp. 1311–1324, Jun. 2023.

[4] W. Chen, Y. X. Yan, and Y. Qi *et al*, "Recent Development of Aircraft Electric Propulsion System: A Technical Review," *CES Trans. on Electr. Mach. and Syst.*, vol. 9, no. 1, pp. 115–130, Mar. 2025.

[5] Q. X. Gao, X. L. Wang, and Z. Q. Deng *et al*, "Loss Calculation, Analysis, and Separation Method of 550 000 r/min Ultrahigh-speed Permanent Magnet Motor," *IEEE Trans. on Ind. Electron.*, vol. 70, no. 4, pp. 3471–3481, Apr. 2023.

[6] Y. X. Wang, J. H. Ji, and J. Li *et al*, "Analysis and Suppression of Circulating Current Loss of High-speed Permanent Magnet Motor," *Chin. J. of Elect. Eng.*, doi: 10.23919/CJEE.2024.000070.

[7] Y. Duan, and D. M. Ionel, "A Review of Recent Developments in Electrical Machine Design Optimization Methods with a Permanent-magnet Synchronous Motor Benchmark Study," *IEEE Trans. on Ind. Appl.*, vol. 49, no. 3, pp. 1268–1275, May-Jun. 2013.

[8] F. Dubas, and A. Rahideh, "Two-dimensional Analytical Permanent-magnet Eddy-current Loss Calculations in Slotless PMSM Equipped with Surface-inset Magnets," *IEEE Trans. on Magn.*, vol. 50, no. 3, pp. 54–73, Mar. 2014.

[9] R. Wrobel, A. Mlot, and P. H. Mellor, "Contribution of End-winding Proximity Losses to Temperature Variation in Electromagnetic Devices," *IEEE Trans. on Ind. Electron.*, vol. 59, no. 2, pp. 848–857, Feb. 2012.

[10] S. Iwasaki, R. Deodhar, and Y. Liu *et al*, "Influence of PWM on the Proximity Loss in Permanent-magnet Brushless AC Machines," *IEEE Trans. on Ind. Appl.*, vol. 45, no. 4, pp. 1359–1367, May 2009.

[11] J. A. Ferreira, "Improved Analytical Modeling of Conductive Losses in Magnetic Components," *IEEE Trans. on Power Electron.*, vol. 9, no. 1, pp. 127–131, Jan. 1994.

[12] L. J. Wu, Z. Q. Zhu, and D. Staton *et al*, "Analytical Model of Eddy Current Loss in Windings of Permanent-magnet Machines Accounting for Load," *IEEE Trans. on Magn.*, vol. 48, no. 7, pp. 2138–2151, Jul. 2012.

[13] D. Golovanov, A. Galassini, and T. Transi *et al*, "Analytical Methodology for Eddy Current Loss Simulation in Armature Windings of Synchronous Electrical Machines with Permanent Magnets," *IEEE Trans. on Ind. Electron.*, vol. 69, no. 10, pp. 9761–9770, Oct. 2022.

[14] S. L. Xu, and H. L. Ren, "Analytical Computation for AC Resistance and Reactance of Electric Machine Windings in Ferromagnetic Slots," *IEEE Trans. on Energy Convers.*, vol. 33, no. 4, pp. 1855–1864, Dec. 2018.

[15] Y. Y. Wang, J. Pries, and K. Zhou *et al*, "Computationally Efficient AC Resistance Model for Stator Winding with Rectangular Conductors," *IEEE Trans. on Magn.*, vol. 56, no. 4, pp. 1–9, Apr. 2020.

[16] P. Mellor, R. Wrobel, and N. Simpson, "AC Losses in High Frequency Electrical Machine Windings Formed from Large Section Conductors," in *Proc. of 2014 IEEE Energy Conversion Congress and Exposition (ECCE)*, Pittsburgh, PA, USA, Sept. 2014, pp. 5563–5570.

[17] A. Cavagnino, "Accuracy-enhanced Algorithms for the Slot Leakage Inductance Computation of Double-layer Windings," *IEEE Trans. on Ind. Appl*., vol. 53, no. 5, pp. 4422–4430, Sep.-Oct. 2017.

[18] D. Golovanov, and C. Gerada, "Analytical Methodology for Modelling of Circulating Current Loss in Synchronous Electrical Machines with Permanent Magnets," *IEEE Trans. on Energy Convers.*, vol. 37, no. 1, pp. 220–231, Mar. 2022.

[19] A. Lehikoinen, N. Chiodetto, and E. Lantto *et al*, "Monte Carlo Analysis of Circulating Currents in Random-wound Electrical Machines," *IEEE Trans. on Magn.*, vol. 52, no. 8, pp.1–12, Aug. 2016.

[20] A. Fatemi, D. M. Ionel, and N. A. O. Demerdash *et al*, "Computationally Efficient Strand Eddy Current Loss Calculation in Electric Machines," *IEEE Trans. on Ind. Appl.*, vol. 55, no. 4, pp. 3479–3489, Jul.-Aug. 2019.

[21] N. Taran, D. M. Ionel, and V. Rallabandi *et al*, "An Overview of Methods and a New Three-dimensional Fea and Analytical Hybrid Technique for Calculating AC Winding Losses in PM Machines," *IEEE Trans. on Ind. Appl*., vol. 57, no. 1, pp. 352–362, Jan.-Feb. 2021.

[22] K. Yamazaki, T. Furuhashi, and H. Y. Yui *et al*, "Analysis and Reduction of Circulating Current Loss of Armature Wires in Permanent Magnet Synchronous Machines," *IEEE Trans. on Ind. Appl.*, vol. 55, no. 6, pp. 5888–5896, Nov.-Dec. 2019.

[23] A. Bardalai, D. Gerada, and D. Golovanov *et al*, "Reduction of Winding AC Losses by Accurate Conductor Placement in High Frequency Electrical Machines," *IEEE Trans. on Ind. Appl.*, vol. 56, no. 1, pp. 183–193, Jan.-Feb. 2020.

[24] D. A. Gonzalez, and D. M. Saban, "Study of the Copper Losses in a High-speed Permanent-magnet Machine with Form-wound Windings," *IEEE Trans. on Ind. Electron.*, vol. 61, no. 6, pp. 3038–3045, Jun. 2014.

[25] G. Volpe, M. Popescu, and L. di Leonardo *et al*, "Efficient Calculation of PWM AC Losses in Hairpin Windings for Synchronous BPM Machines," in *Proc. of 2021 IEEE International Electric Machines & Drives Conference (IEMDC)*, Hartford, CT, USA, May 2021, pp. 1–5.

[26] X. Y. Chen, H. Y. Fang, and X. G. Fan *et al*, "Suppression of Winding AC Copper Loss in High-speed Electrical Machines by a Practical Transposition Technique," *IEEE Trans. on Ind. Appl.*, vol. 58, no. 6, pp. 7121–7130, Nov.-Dec. 2022.

[27] S.-H. Park, J.-W. Chin, and K.-S. Cha *et al*, "Investigation of AC Copper Loss Considering Effect of Field and Armature Excitation on IPMSM with Hairpin Winding," *IEEE Trans. on Ind. Electron.*, vol. 70, no. 12, pp. 12102–12112, Dec. 2023.

[28] X. W. Ju, Y. Cheng, and B. C. Du *et al*, "AC Loss Analysis and Measurement of a Hybrid Transposed Hairpin Winding for EV Traction Machines," *IEEE Trans. on Ind. Electron.*, vol. 70, no. 4, pp. 3525–3536, Apr. 2023.

[29] L. F. Cao, X. G. Fan, and D. W. Li *et al*, "Semi Analytical and Efficient Calculation Method of Eddy Current Loss in Windings of Permanent Magnet Machines based on Fast Finite Element Method," *Trans. of China Electrotech. Soc*., vol. 38, no. 1, pp. 153–165, Feb. 2023.

[30] M. Popescu, and D. G. Dorrell, "Proximity Losses in the Windings of High Speed Brushless Permanent Magnet AC Motors with Single Tooth Windings and Parallel Paths," *IEEE Trans. on Magn.*, vol. 49, no. 7, pp. 3913–3916, Jul. 2013.

[31] G. Volpe, M. Popescu, and F. Marignetti *et al*, "AC Winding Losses in Automotive Traction E-machines: A New Hybrid Calculation Method," in *Proc. of 2019 IEEE Int. Elect. Mach. & Drives Conf. (IEMDC)*, San Diego, CA, USA, May 2019, pp. 2115–2119.

[32] T. E. Hajji, S. Hlioui, and F. Louf *et al*, "Hybrid Model for AC Losses in High Speed PMSM for Arbitrary Flux Density Waveforms," in *Proc. of 2020 Int. Conf. on Elect. Mach. (ICEM)*, Gothenburg, Sweden, Aug. 2020, pp. 2426–2432.

[33] Y. P. Jiang, J. Q. Chen, and H. H. Wang *et al*, "Semi-analytical Method of Form-wound Winding Loss Considering Circulating Current Effect," *IEEE Trans. on Magn.*, vol. 58, no. 2, pp. 1–6, Feb. 2022.

[34] L. Li, X. G. Fan, and Z. R. Liu *et al*, "A Computationally Efficient

Semi-analytical Method for Circulating Current Loss of High Speed Permanent Magnet Machines," *IEEE Trans. on Energy Convers.*, vol. 39, no. 1, pp. 675–687, Mar. 2024.

[35] X. Bian, Y. Zhao, and Y. P. Liang, "Electromagnetic Network Method for Transient Circulating Current Calculation of Stator Transposition Windings in Large Synchronous Compensator based on Equivalence of Local Magnetic Field," *IEEE Trans. on Energy Convers.*, vol. 37, no. 3, pp. 1825–1833, Sep. 2022.

[36] T. M. Luo, M. G. Niasar, and P. Vaessen, "Improved Winding Losses Calculation based on Bessel Functions," *IEEE Trans. on Magn*., vol. 59, no. 6, pp. 1–10, Jun. 2023.

[37] P. Akiki, M. H. Hassan, and M. Bensetti *et al*., "Multiphysics Design of a V-shape IPM Motor," *IEEE Trans. on Energy Convers.*, vol. 33, no. 3, pp. 1141–1153, Sept. 2018.

[38] M. van der Geest, H. Polinder, and J. A. Ferreira *et al*, "Current Sharing Analysis of Parallel Strands in Low-voltage High-speed Machines," *IEEE Trans. on Ind. Electron*., vol. 61, no. 6, pp. 3064–3070, Jun. 2014.

[39] P. Y. Wang, X. J. Wang, and Y. P. Wang, "Physics-informed Machine Learning Based Permanent Magnet Synchronous Motor Temperature Estimation," in *Proc. of 2023 9th International Conference on Mechanical and Electronics Engineering (ICMEE)*, Xi'an, China, 2023, pp. 582–587.

[40] L. Jin, F. Wang, and Q. X. Yang, "Performance Analysis and Optimization of Permanent Magnet Synchronous Motor based on Deep Learning," in *Proc. of 2017 20th International Conference on Electrical Machines and Systems (ICEMS)*, Sydney, NSW, Australia, Aug. 2017, pp. 1–5.

[41] H. T. Shi, L. Guo, and S. Tan *et al*, "Rolling Bearing Initial Fault Detection Using Long Short-term Memory Recurrent Network," *IEEE Access*, vol. 7, pp. 171559–171569, 2019.

[42] X. Zhao, S. G. Wang, and S. X. Niu *et al*, "A Novel High-order-harmonic Winding Design Method for Vernier Reluctance Machine with DC Coils Across Two Stator Teeth," *IEEE Trans. on Ind. Electron*., vol. 69, no. 8, pp. 7696–7707, Aug. 2022.

[43] G. H. Du, N. M. Li, and W. L. Ye *et al*, "Effect of Harmonics on AC Losses and Temperature of Round-wire and Form-wound Windings for HSPMMs," *IEEE Trans. on Transp. Electrification*, vol. 10, no. 3, pp. 6115–6128, Sept. 2024.

[44] D. P. Morisco, S. Kurz, and H. Rapp *et al*, "A Hybrid Modeling Approach for Current Diffusion in Rectangular Conductors," *IEEE Trans. on Magn.*, vol. 55, no. 9, pp. 1–11, Sept. 2019.

[45] A. Arruti, I. Aizpuru, and M. Mazuela *et al*, "Evolution of Classical 1-D-based Models and Improved Approach for the Characterization of Litz Wire Losses," *IEEE Trans. on Power Electron.*, vol. 39, no. 12, pp. 16371–16381, Dec. 2024.

[46] R. Sahu, P. Pellerey, and K. Laskaris, "Eddy Current Loss Model Unifying the Effects of Reaction Field and Non-homogeneous 3-D Magnetic Field," *IEEE Trans. on Magn.*, vol. 56, no. 2, pp. 1–4, Feb. 2020.

[47] W. F. Yu, W. Hua, and Z. H. Zhang *et al*, "Comparative Analysis of AC Copper Loss with Round Copper Wire and Flat Copper Wire of High-speed Stator-PM Flux-switching Machine," *IEEE Trans. on Ind. Appl.*, vol. 58, no. 6, pp. 7131–7142, Nov.-Dec. 2022.

[48] D. Winterborne, S. Jordan, and L. Sjöberg *et al*, "Estimation of AC Copper Loss in Electrical Machine Windings with Consideration of End Effects," in *Prof. of 2020 International Conference on Electrical Machines (ICEM)*, Gothenburg, Sweden, Aug. 2020, pp. 847–853.

[49] L. J. Wu, Z. Q. Zhu, and D. Staton *et al*, "An Improved Subdomain Model for Predicting Magnetic Field of Surface-mounted Permanent Magnet Machines Accounting for Tooth-tips," *IEEE Trans. on Magn.*, vol. 47, no. 6, pp. 1693–1704, Jun. 2011.

[50] L. J. Wu, Z. Q. Zhu, and D. Staton *et al*, "Subdomain Model for Predicting Armature Reaction Field of Surface-mounted Permanent-magnet Machines Accounting for Tooth-tips," *IEEE Trans. on Magn.*, vol. 47, no. 4, pp. 812–822, Apr. 2011.

[51] H. Mahmoud, N. Bianchi, and G. Bacco *et al*, "Nonlinear Analytical Computation of the Magnetic Field in Reluctance Synchronous Machines," *IEEE Trans. on Ind. Appl*., vol. 53, no. 6, pp. 5373–5382, Nov./Dec. 2017.

[52] M. Ojaghi, and S. Nasiri, "Modeling Eccentric Squirrel-cage Induction Motors with Slotting Effect and Saturable Teeth Reluctances," *IEEE Trans. on Energy Convers*., vol. 29, no. 3, pp. 619–627, Sept. 2014.

[53] Z. Djelloul-Khedda, K. Boughrara, and F. Dubas *et al*, "Nonlinear Analytical Prediction of Magnetic Field and Electromagnetic Performances in Switched Reluctance Machines," *IEEE Trans. on Magn*., vol. 53, no. 7, pp. 1–11, Jul. 2017.

[54] W. B. Wang, M. Cheng, and X. L. Li *et al*, "Nonlinear Analytical Solution of Magnetic Field and Performances of a Spoke Array Vernier Permanent Magnet Machine," *IEEE Trans. on Energy Convers*., vol. 36, no. 1, pp. 173–185, Mar. 2021.

[55] Y. Laoubi, M. Dhifli, and G. Verez *et al*, "Open Circuit Performance Analysis of a Permanent Magnet Linear Machine Using a New Hybrid Analytical Model," *IEEE Trans. on Magn*., vol. 51, no. 3, pp. 1–4, Mar. 2015.

[56] A. G. Sarigiannidis, and A. G. Kladas, "Switching Frequency Impact on Permanent Magnet Motors Drive System for Electric Actuation Applications," *IEEE Trans. on Magn.*, vol. 51, no. 3, pp. 1–4, Mar. 2015.

[57] S.-H. Lee, S.-O. Kwon, and J.-J. Lee *et al*, "Characteristic Analysis of Claw-pole Machine Using Improved Equivalent Magnetic Circuit," *IEEE Trans. on Magn.*, vol. 45, no. 10, pp. 4570–4573, Oct. 2009.

[58] D. H. Cao, W. X. Zhao, and J. H. Ji *et al*, "A Generalized Equivalent Magnetic Network Modeling Method for Vehicular Dual-permanent-magnet Vernier Machines," *IEEE Trans. on Energy Convers.*, vol. 34, no. 4, pp. 1950–1962, Dec. 2019.

[59] S. Jiang, G. H. Liu, and W. X. Zhao *et al*, "Modeling and Analysis of Spoke-type Permanent Magnet Vernier Machine based on Equivalent Magnetic Network Method," *Chin. J. of Elect. Eng.*, vol. 4, no. 2, pp. 96–103, Jun. 2018.

[60] Y. Zhu, G. H. Liu, and L. Xu *et al*, "A Hybrid Analytical Model for Permanent Magnet Vernier Machines Considering Saturation Effect," *IEEE Trans. on Ind. Electron.*, vol. 69, no. 2, pp. 1211–1223, Feb. 2022.

[61] S. Ouagued, A. A. Diriye, and Y. Amara *et al*, "A General Framework based on a Hybrid Analytical Model for the Analysis and Design of Permanent Magnet Machines," *IEEE Trans. on Magn.*, vol. 51, no. 11, pp. 1–4, Nov. 2015.

[62] W. Zhao, D. Cao, J. Ji, L. Huang and T. Liu, "A Generalized Mesh-Based Thermal Network Model for SPM Machines Combining Coupled Winding Solution," *IEEE Trans. on Ind. Electron.*, vol. 68, no. 1, pp. 116-127, Jan. 2021.

[63] R. Krüger, P. P. Durán, and T. Gerhard *et al*, "Current Displacement Effects on Copper Losses in PWM Supplied Electrical Machines," *IEEE Trans. on Energy Convers.*, vol. 38, no. 4, pp. 2754–2761, Dec. 2023.

[64] R. Krüger, S. Singh, and P. P. Durán *et al*, "Inverter Control and its Effect on Copper Losses in Electrical Machines Equipped with Hairpin Winding," in *Proc. of 2022 12th International Electric Drives Production Conference (EDPC)*, Regensburg, Germany, Nov. 2022, pp. 1–7.

[65] X. G. Fan, D. W. Li, and W. B. Kong *et al*, "Fast Calculation of Strand Eddy Current Loss in Inverter-fed Electrical Machines," *IEEE Trans. on Ind. Electron*., vol. 70, no. 5, pp. 4640–4650, May 2023.

[66] K. D. Huang, B. C. Ding, and C. Y. Lai *et al*, "Flux Linkage Tracking-based Permanent Magnet Temperature Hybrid Modeling and Estimation for PMSMs with Data-driven-based Core Loss Compensation," *IEEE Trans. on Power Electron.*, vol. 39, no. 1, pp. 1410–1421, Jan. 2024.

[67] J. Y. Zhao, H. Guo, and L. K. Wang *et al*, "Computer Modeling of the Eddy Current Losses of Metal Fasteners in Rotor Slots of a Large Nuclear Steam Turbine Generator Based on Finite-element Method and Deep Gaussian Process Regression," *IEEE Trans. on Ind. Electron.*, vol. 67, no. 7, pp. 5349–5359, Jul. 2020.

[68] Z. Q. Yang, H. H. Dong, and J. Man *et al*, "Online Deep Learning for High-speed Train Traction Motor Temperature Prediction," *IEEE Trans. on Transp. Electrification*, vol. 10, no. 1, pp. 608–622, Mar. 2024.

[69] P. C. Sun, S. F. Jia, and D. L. Liang *et al*, "A Review on the Development of High-reliability Motor System for Safety-critical Applications—From Redundancy Design Prospective," *IEEE Trans. on Transp. Electrification*, vol. 10, no. 3, pp. 7374–7388, Sep. 2024.

[70] Y. Shimizu, "Automatic Design System with Generative Adversarial Network and Vision Transformer for Efficiency Optimization of Interior Permanent Magnet Synchronous Motor," *IEEE Trans. on Ind. Electron.*, vol. 71, no. 11, pp. 14600–14609, Nov. 2024.

[71] A. Khan, V. Ghorbanian, and D. Lowther, "Deep Learning for Magnetic Field Estimation," *IEEE Trans. on Magn.*, vol. 55, no. 6, pp. 1–4, Jun.

2019.

[72] L. H. Jin, Y. Mao, and X. Q. Wang *et al*, "A Model-based and Data-driven Integrated Temperature Estimation Method for PMSM," *IEEE Trans. on Power Electron.*, vol. 39, no. 7, pp. 8553–8561, July 2024.

[73] W. Kirchgässner, O. Wallscheid, and J. Böcker, "Estimating Electric Motor Temperatures with Deep Residual Machine Learning," *IEEE Trans. on Power Electron.*, vol. 36, no. 7, pp. 7480–7488, Jul. 2021.

[74] S.-H. Park, K.-O. Kim, and M.-S. Lim, "Computationally Efficient Estimation of PWM-induced Iron Loss of PMSM Using Deep Transfer Learning," *IEEE Trans. on Magn.*, vol. 59, no. 11, pp. 1–5, Nov. 2023.

[75] W. X. Zhao, Y. Wang, and J. H. Ji *et al*, "Reduced Order Model Coupling Frequency Domain Method for Calculation of Core Loss in SPM Machine Considering PWM Current Harmonics," *IEEE Trans. on Ind. Electron.*, vol. 72, no. 1, pp. 220–229, Jan. 2025.

[76] C. Chi, F. Yang, and Z. X. Ren, "Reduced Order Model based on Combined POD/LDEIM-Q for Nonlinear Thermoelectric Coupling," *IEEE Trans. on Magn.*, vol. 58, no. 9, pp. 1–4, Sept. 2022.

[77] Z. Li, J. J. Shan, and U. Gabbert, "Development of Reduced Preisach Model Using Discrete Empirical Interpolation Method," *IEEE Trans. on Ind. Electron.*, vol. 65, no. 10, pp. 8072–8079, Oct. 2018.

Kaiwei He received the B.S. degree in automation from Dalian University of Technology, Dalian, China, in 2021. She is currently working toward the M.S. degree in control science and engineering at Jiangsu University.

Her current research interests include modeling and calculation of high frequency AC copper loss of PMSM systems.

Wenxiang Zhao (M'08-SM'14) received the B.S. and M.S. degrees in electrical engineering from Jiangsu University, Zhenjiang, China, in 1999 and 2003, respectively, and the Ph.D. degree in electrical engineering from Southeast University, Nanjing, China, in 2010.

From 2008 to 2009, he was a Research Assistant with the Department of Electrical and Electronic Engineering, University of Hong Kong, Hong Kong. From 2013 to 2014, he was a Visiting Professor with the Department of Electronic and Electrical Engineering, University of Sheffield, Sheffield, U.K. Currently, he is a Professor with the School of Electrical and Information Engineering, Jiangsu University, and also with the School of Electric Power Engineering, Nanjing Institute of Technology. He has authored and coauthored over 200 papers published in various IEEE TRANSACTIONS. His current research interests include electric machines and control.

Zhongze Wu (S'15-M'18-SM'22) received the B.Eng. and M.S. degrees in electrical engineering from Southeast University, Nanjing, China, in 2010 and 2013, respectively, and the Ph.D. degree in electrical and electronic engineering from The University of Sheffield, Sheffield, U.K., in January 2017.

Since March 2021, he has been with School of Electrical Engineering, Southeast University, Nanjing, China, where he is currently a professor. His major research interests include the advanced electrical machines and drives for electric propulsion systems.

From January 2017 to August 2018, he was with Warwick Manufacturing Group (WMG), University of Warwick, Coventry, U.K., as a research fellow in electrical machines. From August 2018 to August 2020, he was with the Institute for Advanced Automotive Propulsion Systems (IAAPS), Department of Mechanical Engineering, University of Bath, Bath, U.K., as a Prize Fellow, where he was a Lecturer between August 2020 and January 2021.

Jinghua Ji received the B.S., M.S., and Ph.D. degrees in electrical engineering from Jiangsu University, Zhenjiang, China, in 2000, 2003, and 2009, respectively.

Since 2000, she has been with the School of Electrical and Information Engineering, Jiangsu University, where she is currently a professor. From 2013 to 2014, she was a Visiting Scholar with the Department of Electronic and Electrical Engineering, University of Sheffield, Sheffield, U.K. She has authored or coauthored over 50 technical papers in these areas. Her research interests include electrical machines and motor drives.